

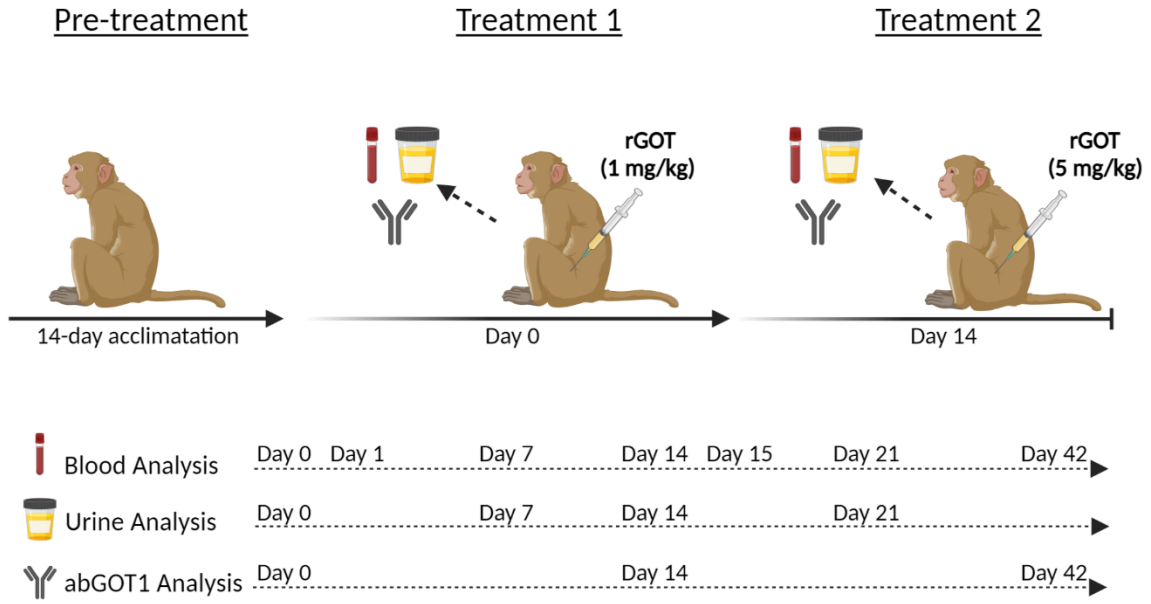
Supplemental information

Preclinical validation of human recombinant glutamate-oxaloacetate transaminase for the treatment of acute ischemic stroke

María Pérez-Mato, Antonio Dopico-López, Yunus Akkoc, Sonia López-Amoedo, Clara Correa-Paz, María Candamo-Lourido, Ramón Iglesias-Rey, Esteban López-Arias, Ana Bugallo-Casal, Andrés da Silva-Candal, Susana B. Bravo, María del Pilar Chantada-Vázquez, Susana Arias, María Santamaría-Cadavid, Ana Estany-Gestal, Ahlem Zaghmi, Marc A. Gauthier, María Gutiérrez-Fernández, Abraham Martín, Jordi Llop, Cristina Rodríguez, Ángeles Almeida, Martina Migliavacca, Ester Polo, Beatriz Pelaz, Devrim Gozuacik, Naouale El Yamani, Tanima SenGupta, Elise Rundén-Pran, José Vivancos, Mar Castellanos, Exuperio Díez-Tejedor, Tomás Sobrino, Aharon Rabinkov, David Mirelman, José Castillo, and Francisco Campos

SUPPLEMENTARY FIGURES

A



B

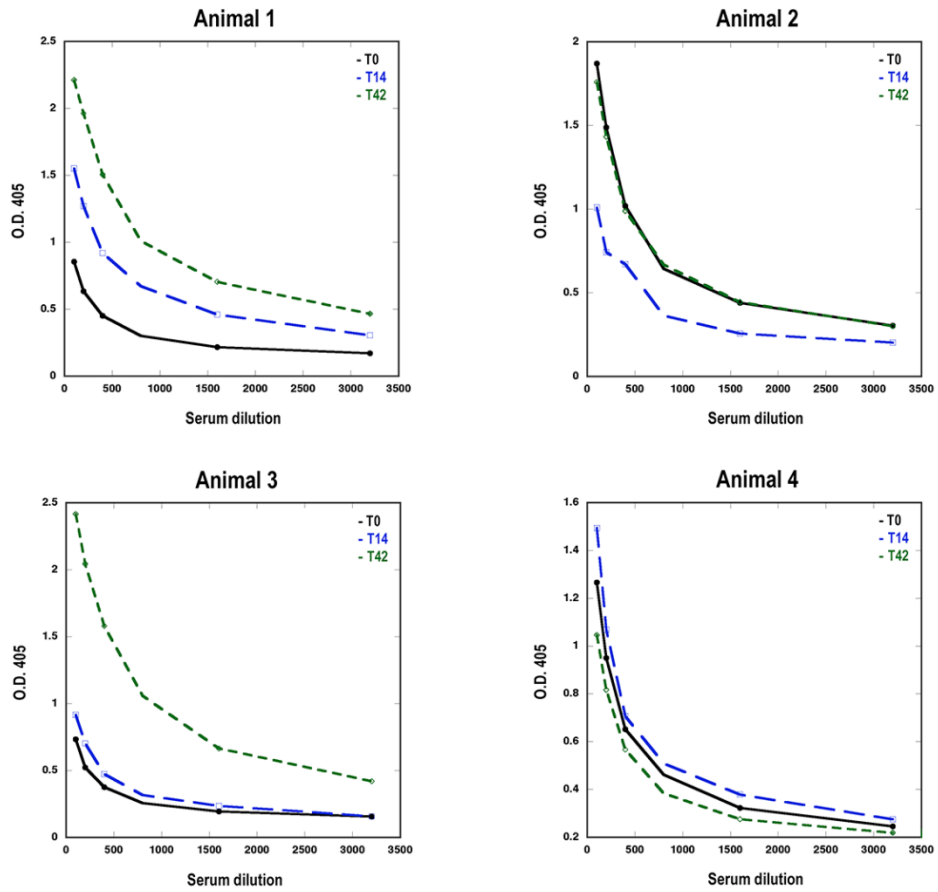
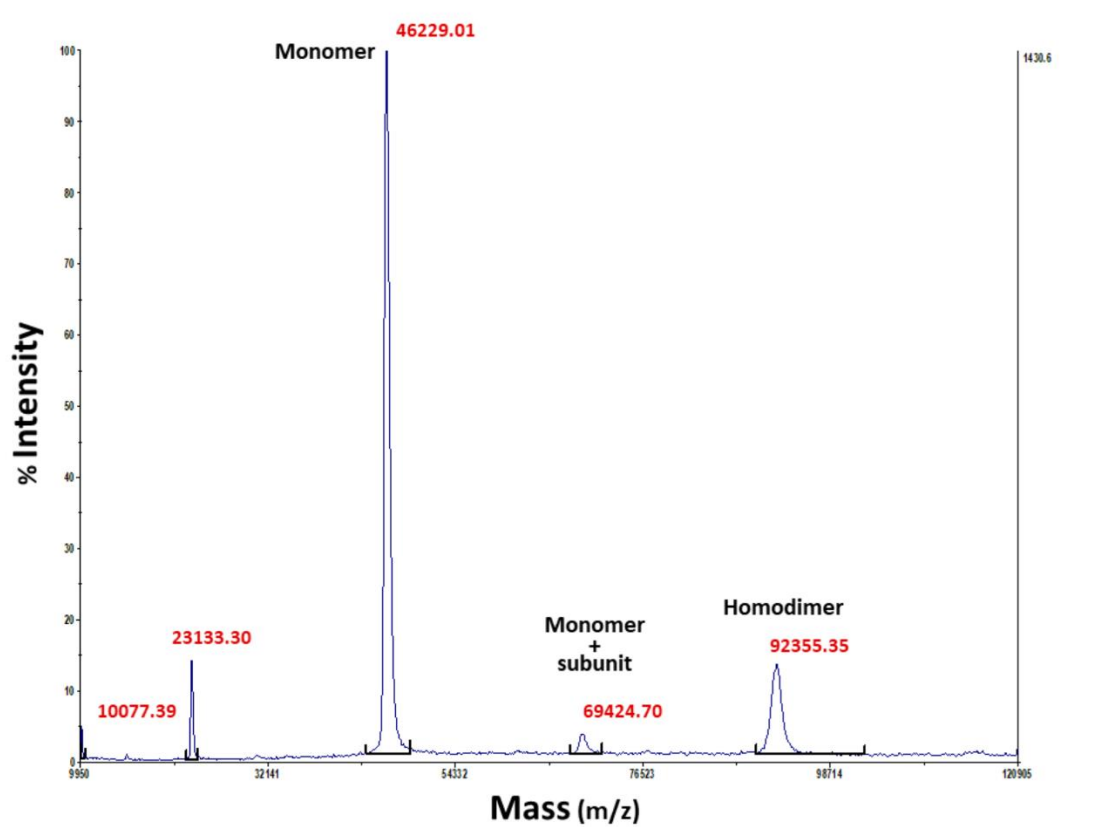


Figure S1. Safety analysis of rGOT in NHPs, Related to Figure 1. (A). Representation of the safety analysis of rGOT in NHPs. Animals received (*i.v.*) an initial dose of 1 mg/kg rGOT and a second dose of 5 mg/kg on day 14 after the first dose ($n = 4$). Blood analysis parameters (hematological, hemostasis, and biochemical) were evaluated on days 0, 1, 7, 14, 15, 21, and 42. Urine analysis was performed on days 0, 7, 14, and 21. Immunogenicity analysis, used to determine the development of antibodies against rGOT, was conducted on days 0, 14, and 42 of the follow-up period. (B). Analysis of antibodies against rGOT in NHP serum in the four animals included in the study. The serum was analyzed undiluted and diluted to the following ranges (1:250, 1:500, 1:500, and 1:3000). GraphPad Prism software (v.8.3.0) was used for representation of graphs. abGOT, antibodies against rGOT; *i.v.*, intravenous; NHP, non-human primate; rGOT, human recombinant form of glutamate-oxaloacetate transaminase 1. BioRender (<https://biorender.com/>) was used for creating the figures.

A



B

MAPPVFAEVPQAQPVLVFKLTADFREDPDPKRVNLGVGAYRTDDCHPWVLPVVKKVEQKIANDNSLNHEYLPILGLAEFRSCASR
 LALGDDSPALKEKRVGGVQSLGGTGALRIGADFLARWYNGTNNKNTFPVYVSSPTWENHNAVFSAAAGFKDIRSYRYWDAEKRLDLDLQ
 GFLNDLENAPPEFSIVVLHACAHNPTGIDPTPEQWKQIASVMKHRFLFPFFDSAYQGFASGNLERDAWAIRYFVSEGFEFFCAQSF
 KNFGLYNERVGNLTVVGKEPESILQVLSQMEKIVRITWSNPPAQGARIVASTLSNPELFEWTFGNVKTMDRILITMRSELRLARLEA
 LKTPGTWNHITDQIGMFSFTGLNPKQVEYLVNEKHIYLLPSGRINVSGLTTKNLDYVATSIHEAVTKIQ

UniProt sequence from GOT1 protein. In green are shown the peptides identified with 99% of confidence using ProteinPilot, in yellow peptides with only 50% of confidence and in red peptides with less than 10% of confidence.

C

Unused ^a	% cov(95%) ^b	Accession number	Uniprot code	Protein name	Species	Peptides identified
181.07	91	sp P17174 AATC_HUMAN	P17174	Glutamate Oxalacetate Transaminase (GOT1)	Human	1309

Compiled list of parameters of the GOT1 protein identified from ProteinPilot software

^a Unused column is an identification score equivalent to the score of other databases such as Mascot. In this identification a score higher than 0.07 corresponds to a 99% of confidence. ^b % Coverage (95%) is the sequence coverage pertaining to only high confidence peptides (95% or greater confidence).

Figure S2. Proteomic characterization of rGOT, Related to Figure 1 and STAR Methods.

(A), MALDI-TOF analysis of the manufactured human rGOT. In accordance with the human form (EC 2.6.1.1), MALDI-TOF MS analysis indicated that the produced enzyme consists of a

homodimer polypeptide (92 kDa), formed by two identical monomers (46 kDa). **(B)**, Protein digestion and identification using LC-MS/MS. **(C)**, Mass spectrometry from LC-MS/MS submitted to the human specific database (UniProt) search. More than 1300 peptides identical to those found in the UniProt database for hGOT protein (see peptides in green) were identified; this represents >91% of the sequence covered of the GOT amino acid sequence (peptides in yellow were only 90% identical, and red peptides were only 10% identical to the GOT protein UniProt sequence). LC-MS/MS, liquid chromatography with tandem mass spectrometry; h, human; MALDI-TOF MS, matrix-assisted laser desorption/ionization-time of flight; rGOT, human recombinant form of glutamate-oxaloacetate transaminase 1.

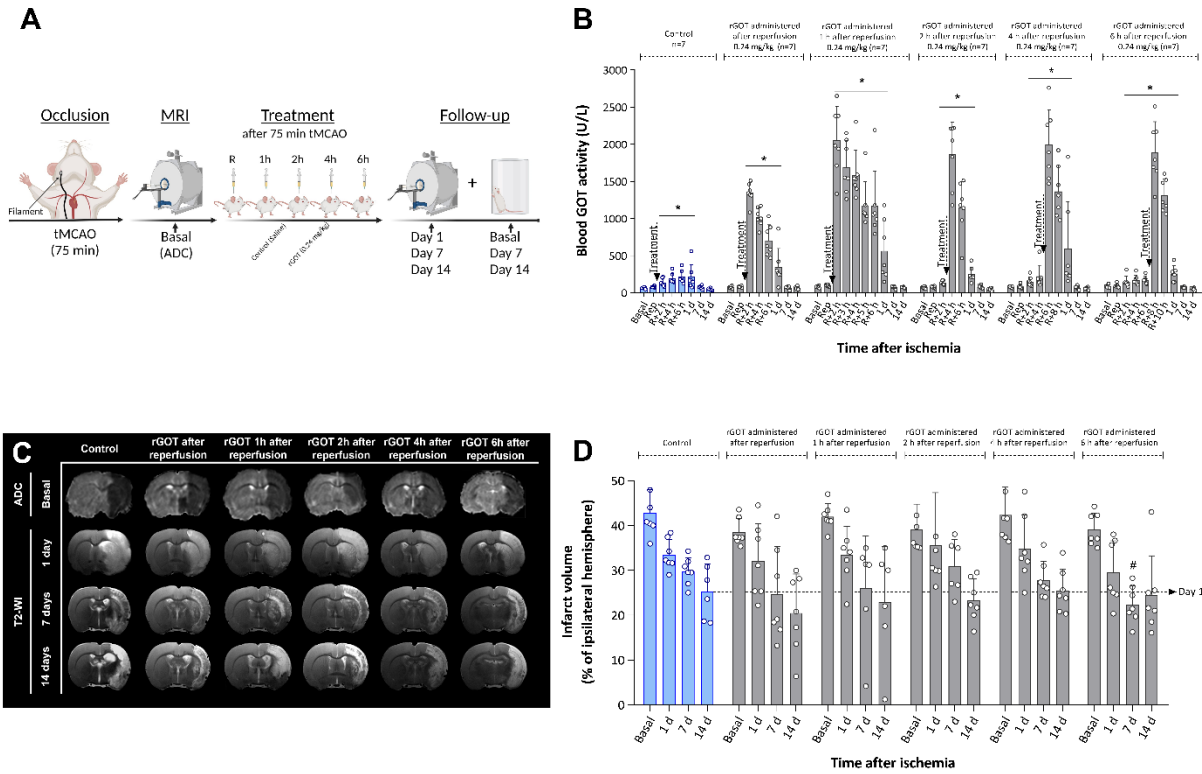


Figure S3. Therapeutic time-window study of rGOT in ischemic rats, Related to Figure 2.

(A), Schematic representation of the experimental design. Treatment with rGOT 0.24 mg/kg was administered as a single *i.v.* bolus immediately and 1, 2, 4, and 6 h after artery reperfusion (75 min after cerebral occlusion) in independent groups of ischemic animals. Ischemic lesions were measured by MRI on day 0 by ADC maps (during cerebral artery occlusion) and on days 1, 7, and 14 after ischemia induction by T2-maps. Basal lesion assessment on day 0 was used to confirm similar lesion volumes (35–45%) in all included animals before treatment administration. (B), Time course of blood GOT activity in ischemic rats. (C), MRI analysis of ischemic evolution. (D), Infarct size assessment in ischemic rats. Ischemic lesions are represented as % adjusted to the ipsilateral hemisphere. The dashed line represents the infarct volume 14 days after ischemia in the control group which was used as a reference. Data are shown as the mean \pm standard deviation. * $p < 0.05$ compared with the basal. # $p < 0.05$ compared with the control group at same time-point. The data were analyzed using SPSS statistical software (v19.0) and GraphPad Prism software (v.8.3.0) for representation of graphs. The criterion for statistical significance was set at $p < 0.05$. The Shapiro–Wilk test was used to determine whether the data were normally distributed. Based on the results of normality tests and the sample size, statistical analysis was performed using non-

parametric tests, Wilcoxon test for paired data, and Mann–Whitney test for unpaired data. ADC, apparent diffusion coefficient; *i.v.*, intravenous; MRI, magnetic resonance imaging; R/Rep, reperfusion rate; rGOT, human recombinant form of glutamate-oxaloacetate transaminase 1; tMCAO, transient middle cerebral artery occlusion; T2-WI, T2-weighted imaging. BioRender (<https://biorender.com/>) was used for creating the figures.

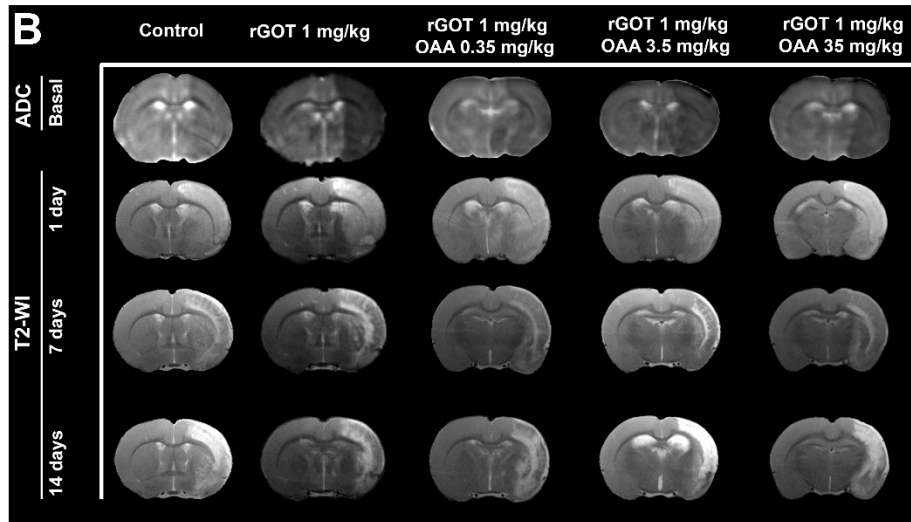
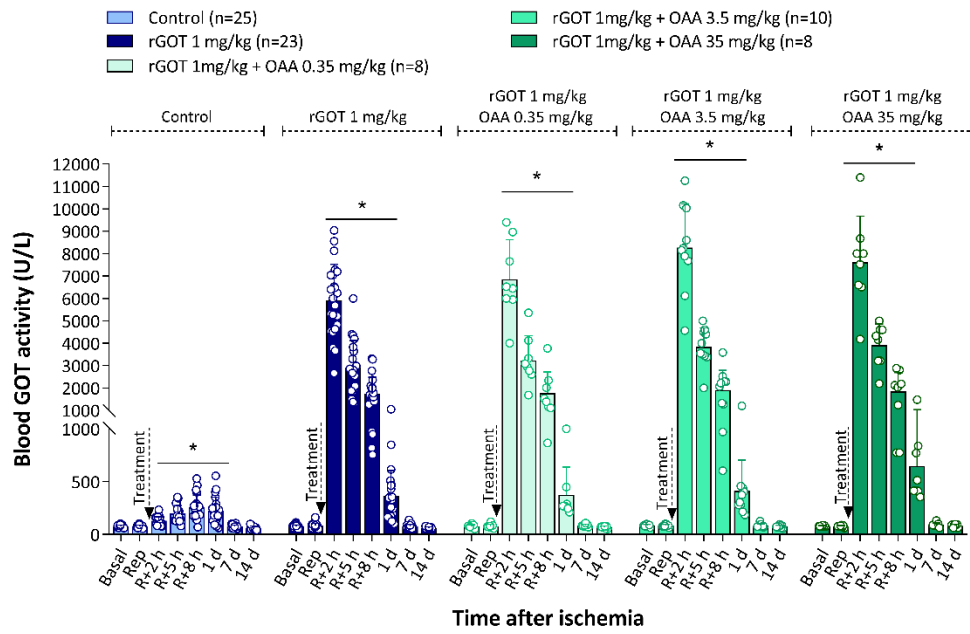
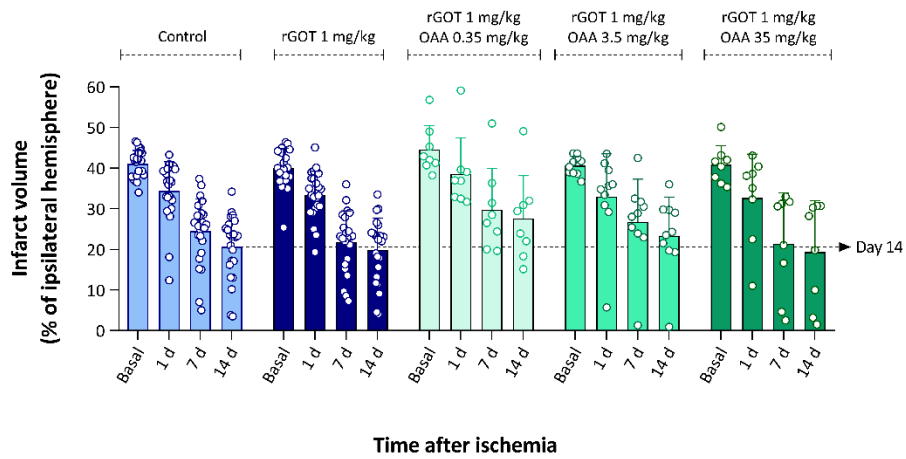
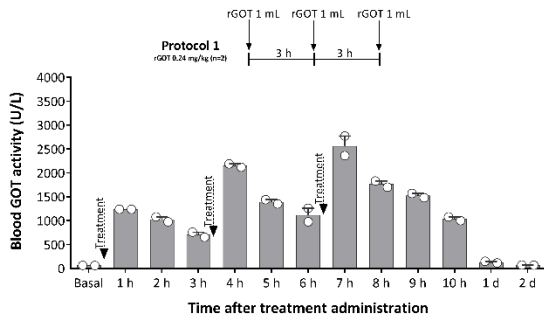
A**C**

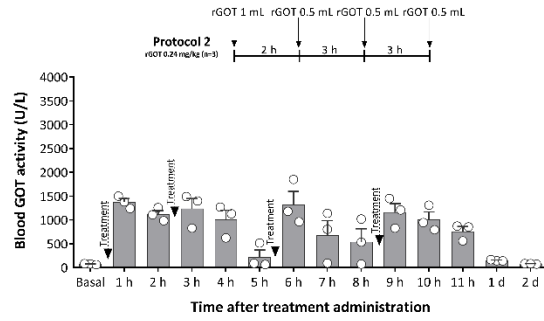
Figure S4. Therapeutic effects of rGOT-supplemented oxaloacetic acid in rats with ischemia, Related to Figure 2. (A) Time course of blood GOT activity in ischemic rats. OAA acid (0.35, 3.5, and 35 mg/kg) in combination with rGOT (1 mg/kg) were administered as a single *i.v.* bolus immediately after arterial reperfusion (75 min after cerebral occlusion) in independent groups of ischemic animals. Ischemic lesions were measured by MRI on day 0 by ADC maps (during cerebral artery occlusion) and on days 1, 7, and 14 after ischemia induction by T2-maps. Basal lesion assessment on day 0 was used to confirm similar lesion volumes (35–45%) in all included animals before treatment administration. (B), MRI analysis of ischemic evolution. (C), Infarct size assessment in ischemic rats. Ischemic lesions are represented as % adjusted to the ipsilateral hemisphere. The dashed line represents the infarct volume at 14 days after ischemia in the control group, which was used as a reference to determine the effect of treatments. Data are shown as the mean \pm standard deviation of the mean. $p^* < 0.05$ compared with the basal. The data were analyzed using SPSS statistical software (v19.0) and GraphPad Prism software (v.8.3.0) for representation of graphs. BioRender (<https://biorender.com/>) was used for creating the figures. The criterion for statistical significance was set at $p < 0.05$. The Shapiro–Wilk test was used to determine whether the data were normally distributed. Based on the results of normality tests and the sample size, statistical analysis was performed using non-parametric tests, Wilcoxon test for paired data, and Mann–Whitney test for unpaired data. ADC, apparent diffusion coefficient; *i.v.*, intravenous; MRI, magnetic resonance imaging; R/Rep, reperfusion rate; tMCAO, transient middle cerebral artery occlusion; rGOT, human recombinant form of glutamate-oxaloacetate transaminase 1; OAA, oxaloacetic acid; T2-WI, T2-weighted imaging.



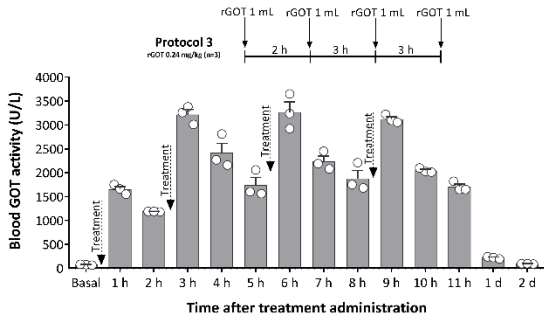
A Consecutive rGOT injections (healthy animals)



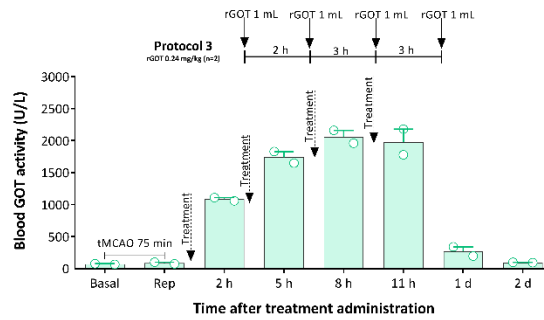
B Consecutive rGOT injections (healthy animals)



C Consecutive rGOT injections (healthy animals)



D Consecutive rGOT injections (ischemic animals)



E Consecutive rGOT injections (NHPs)

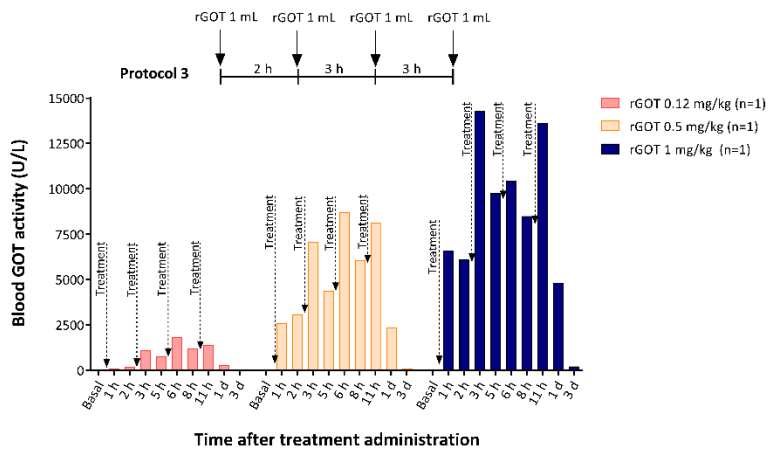


Figure S5. Analysis of consecutive doses of rGOT on blood GOT activity in rats and NHPs, Related to Figure 2. (A), Protocol 1, which was evaluated in healthy animals, consisted of the administration *i.v.* of three doses of 1 mL (0.24 mg/kg), separated by an interval of 3 h. This protocol was discarded because the increase in GOT activity in the blood was not sustained after an initial interval of 3 h. (B), Protocol 2, evaluated again in healthy animals, consisted of the administration of an initial dose of 1 mL (0.24 mg/kg), followed by three consecutive doses (0.5 mL; 0.24 mg/kg), divided in intervals of 2, 3, and 3 h after the first dose. This protocol was discarded as well, because the increase of GOT activity in blood was not sustained when a volume of 0.5 mL was used in the three last administrations. (C), Protocol 3 consisted of four doses of 1 mL of rGOT (0.24 mg/kg) administered in a period of 8 h, with intervals of 2, 3, and 3 h after the first dose. Using this protocol, we were able to maintain a sustained increase in GOT activity for at least 12 h after the first administration. (D), The sustained increase in GOT activity of the selected protocol 3 was validated in ischemic animals. (E), Protocol 3 was also evaluated in three independent healthy NHP models using three increasing doses (0.12, 0.5, and 1 mg/kg). Data are shown as the mean \pm standard deviation of the mean. The data were analyzed using SPSS statistical software (v19.0) and GraphPad Prism software (v.8.3.0) for representation of graphs. *i.v.*, intravenous; NHP, non-human primate; Rep, reperfusion; rGOT, human recombinant form of glutamate-oxaloacetate transaminase 1; tMCAO, transient middle cerebral artery occlusion. BioRender (<https://biorender.com/>) was used for creating the figures.

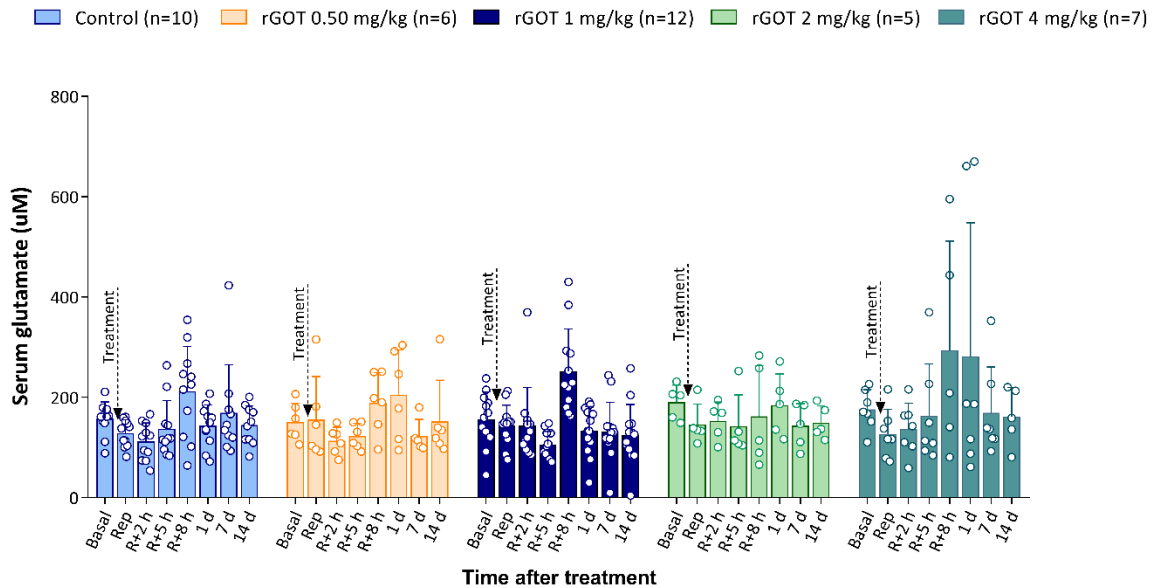
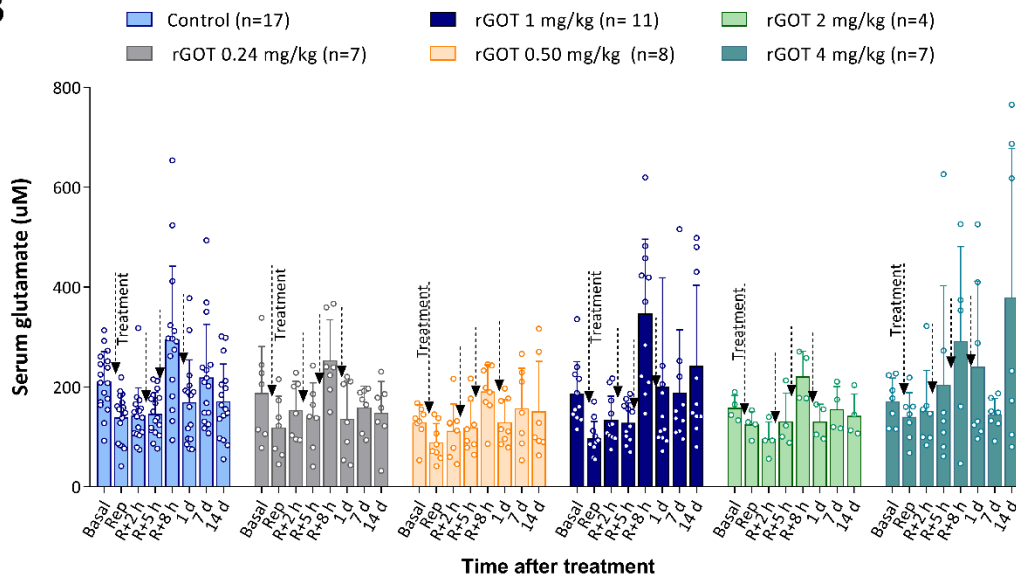
A**B**

Figure S6. Blood glutamate levels in ischemic animals, Related to Figure 2 and Figure 3. (A), Time course of blood glutamate levels in rats with severe ischemia (75 min) rats treated with a single dose of 0.24 to 4 mg/kg of rGOT, from Fig. 2. **(B),** Time course of blood glutamate levels in rats with severe ischemia (75 min) rats treated with four doses dose of 0.24 to 4 mg/kg of rGOT, from Fig. 3. Data are shown as the mean \pm standard deviation of the mean. The data were analyzed

using SPSS statistical software (v19.0) and GraphPad Prism software (v.8.3.0) for representation of graphs. BioRender (<https://biorender.com/>) was used for creating the figures. rGOT, human recombinant form of glutamate-oxaloacetate transaminase

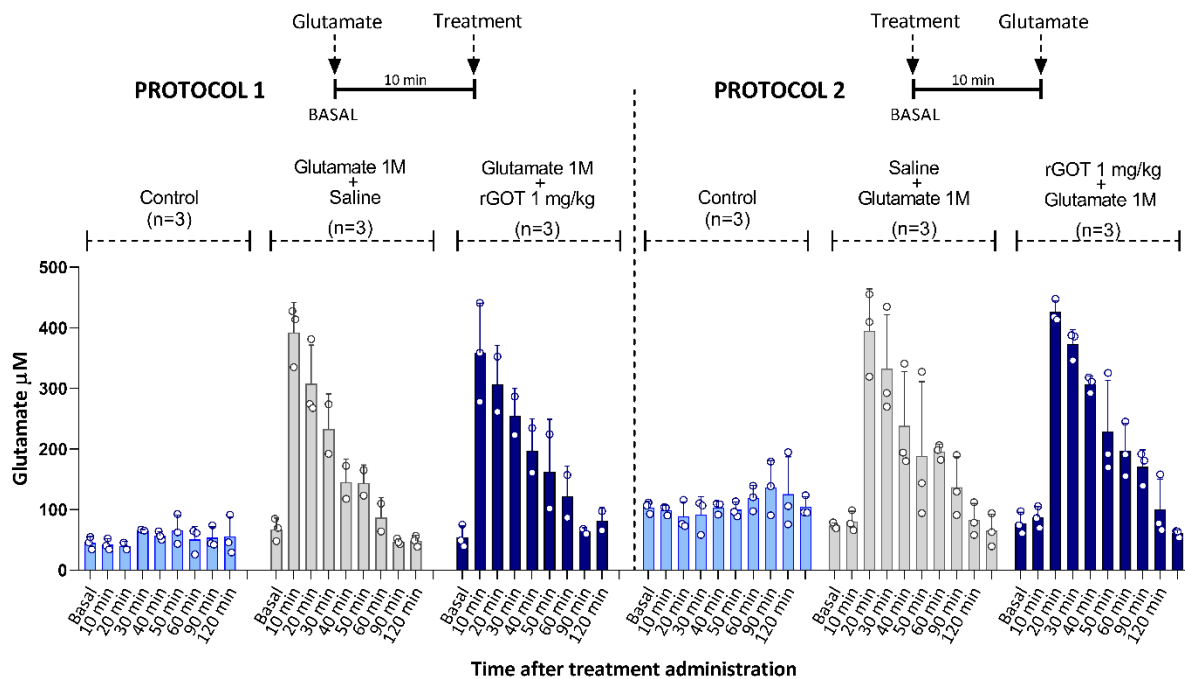


Figure S7. Effect of rGOT treatment on the blood-induced glutamate increase, Related to Figure 2 and Figure 3. An artificial increase of glutamate in healthy animals was induced by injection (*i.v.*) of 1 mL of 1 M glutamate, and the effect of rGOT 1 mg/kg treatment on blood glutamate lowering was evaluated 10 min after glutamate administration (Protocol 1) and 10 min pre-glutamate administration. The control animals were treated with saline. Saline was used as a vehicle in the control group treated with glutamate alone. Data are shown as the mean \pm standard deviation of the mean. The data were analyzed using SPSS statistical software (v19.0) and GraphPad Prism software (v.8.3.0) for representation of graphs. BioRender (<https://biorender.com/>) was used for creating the figures. *i.v.*, intravenous; rGOT, human recombinant form of glutamate-oxaloacetate transaminase 1.

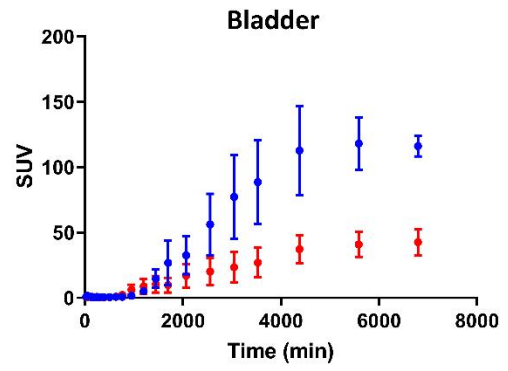
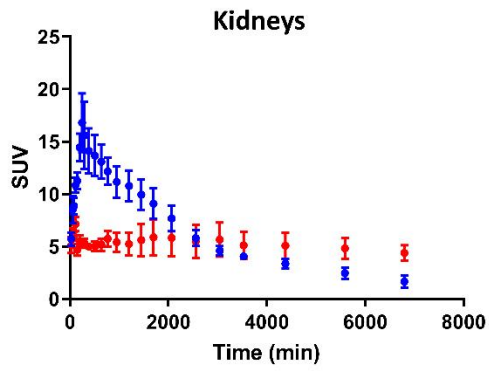
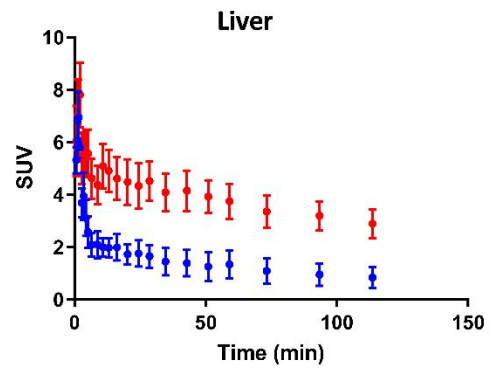
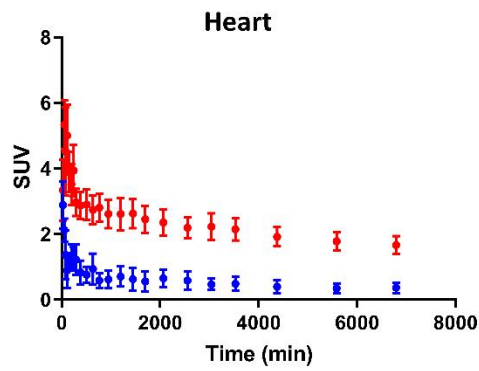
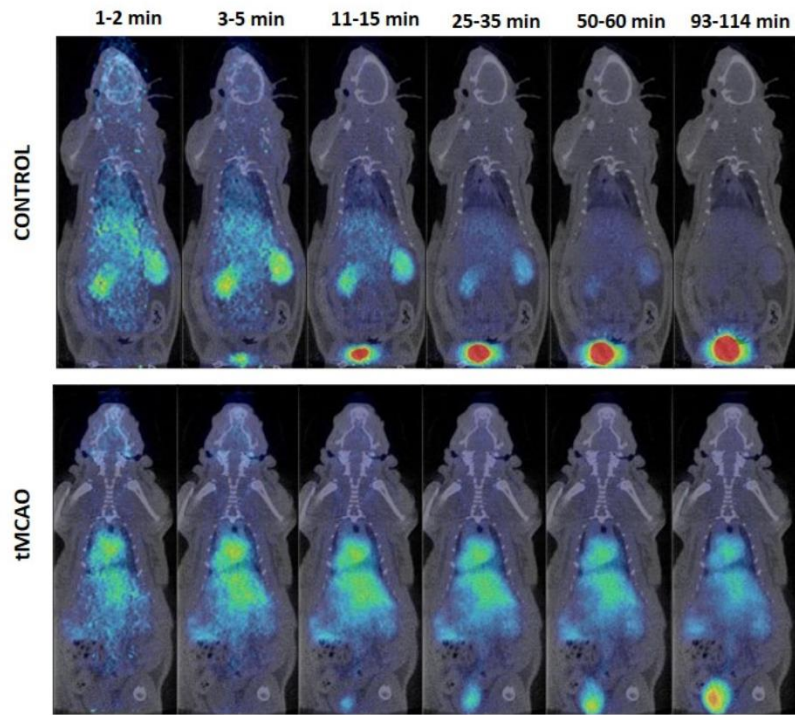


Figure S8. Whole-body distributions of [¹⁸F]rGOT, Related to Figure 6. PET images (maximum intensity projections, coronal views) obtained at different time points after *i.v.* administration of [¹⁸F]rGOT (1 mg/kg) in control (top) and tMCAO (bottom) rats. PET images have been co-registered with CT images (representative slices) of the same animal for proper localization of the radioactive signal. Time-activity curves in the heart, liver, kidneys, and bladder after *i.v.* administration of [¹⁸F]GOT in control (blue) and MCAO (red) rats. Data are shown as mean ± standard deviation of the mean. The data were analyzed using SPSS statistical software (v19.0) and GraphPad Prism software (v.8.3.0) for representation of graphs. BioRender (<https://biorender.com/>) was used for creating the figures. CT, computed tomography; *i.v.*, intravenous; PET, positron emission tomography; rGOT, human recombinant form of glutamate-oxaloacetate transaminase 1; SUV, standardized uptake values; tMCAO, transient middle cerebral artery occlusion.

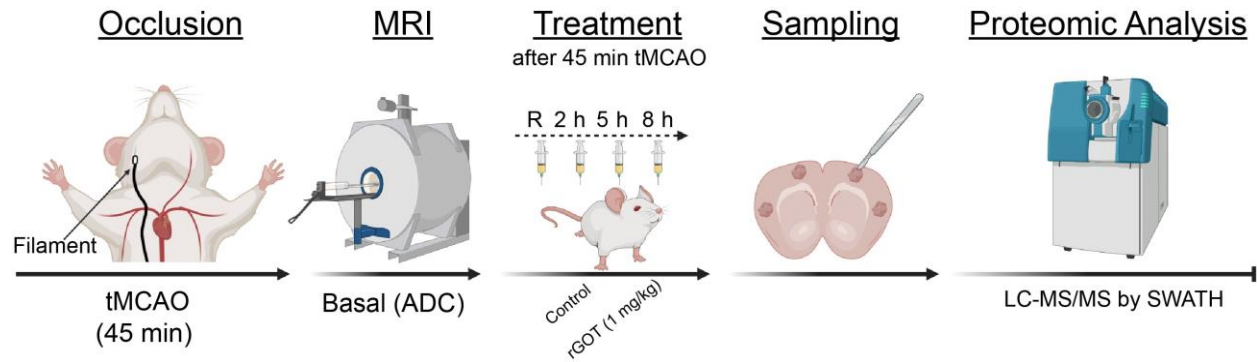
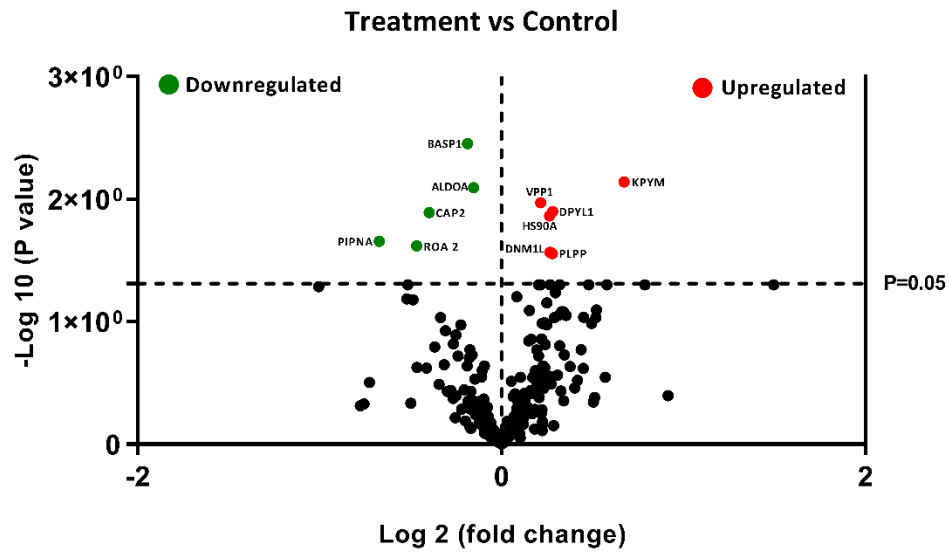


Figure S9. Proteomic analysis of GOT in the brain, Related to Figure 6. Schematic representation of the proteomic analysis of GOT in the brains of ischemic animals. Ischemic animals subjected to 45 min of cerebral ischemia were treated with saline (control) or the selected protective dosage consisting of four doses of rGOT (1 mg/kg) administered immediately after reperfusion (R) and at 2, 5, and 8 h. Twenty-four hours after ischemic induction, the brains of animals were perfused, and the tissue was analyzed by quantitative LC-MS/MS by SWATH-MS. LC-MS/MS, liquid chromatography with tandem mass spectrometry; SWATH-MS, sequential window acquisition of all theoretical mass spectra; rGOT, human recombinant form of glutamate-oxaloacetate transaminase 1. BioRender (<https://biorender.com/>) was used for creating the figures.

A



B

Protein name	Uniprot code	Gene name	p-value	Fold change
Pyruvate kinase	P11980	KPYM	0.007	1.59
Dihydropyrimidinase-related protein 1	Q62950	DPYL1	0.012	1.21
Dynammin-1-like protein	O35303	DNMI1	0.027	1.20
Heat shock protein HSP 90-alpha	P82995	HS90A	0.013	1.20
Pyridoxal phosphate phosphatase	Q8VD52	PLPP	0.027	1.21
V-type proton ATPase	P25286	VPP1	0.01	1.16
Fructose-bisphosphate aldolase A	P05065	ALDOA	0.008	0.89
Brain acid soluble protein	Q05175	BASP1	0.003	0.87
Adenylyl cyclase-associated protein	P52481	CAP2	0.012	0.75
Heterogeneous nuclear ribonucleoproteins A2/B1	A7VJC2	ROA2	0.024	0.72
Phosphatidylinositol transfer protein alpha isoform	P16446	PIPNA	0.022	0.62

C

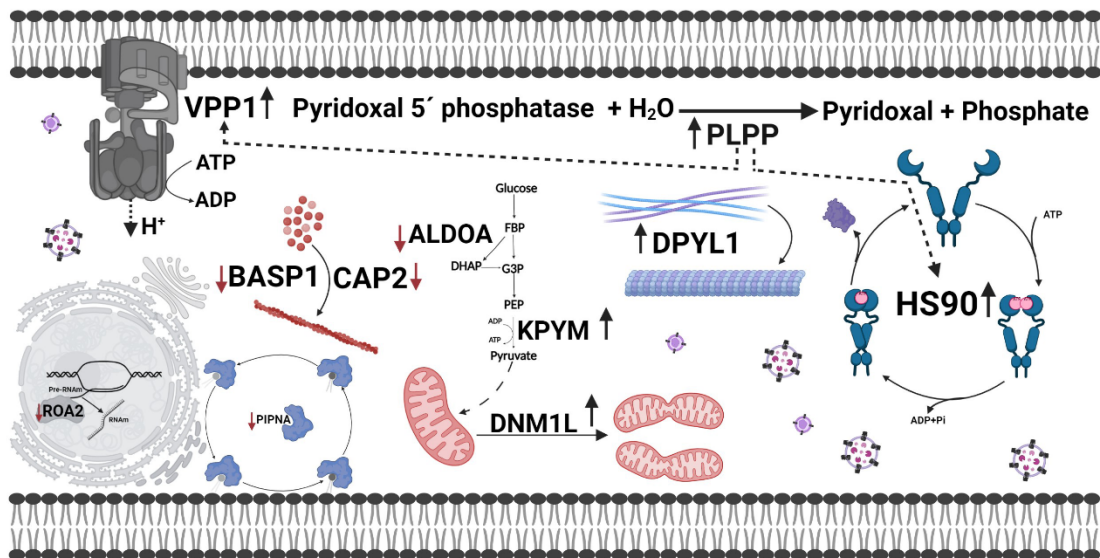


Figure S10. Brain protein expression affected by rGOT treatment, Related to Figure 6. (A), Volcano plot of quantitative proteomics data from brain samples. The volcano plot shows the significantly differentially proteins in the brain according to quantitative proteomics analysis. Proteins are ranked in a volcano plot according to their statistical p value (y-axis) as $-\log_{10}$ and their relative abundance ratio (\log_2 FC) between the treated and control samples (x-axis). Off-centered spots are those that vary the most between both groups. The cut-offs for significant changes are *fold change* >1.5 or <0.8 and $P < 0.05$. Green spots show the downregulated proteins in ischemic animals treated with four doses of rGOT 1 mg/kg compared with control ischemic animals; red spots show the upregulated proteins between both groups. **(B),** Relation of the gene and protein names. Of the proteins affected by rGOT treatment, we observed a significant upregulation of proteins related to cell metabolism and mitochondrial activity, such as DNMI1L,⁴⁰ as well as others involved in ATP hydrolysis, VPP1⁴¹, and many others related to stroke recovery, including KP YM,⁴² PLPP,⁴³ HSP90,⁴⁴ and DPYL1.⁴⁵ Meanwhile, the downregulated proteins, which have been described in other studies, appear to be related to the severity of ischemic lesions and include ALDOA,⁴⁶ ROA2,⁴⁷ and PIPNA.⁴⁸ **(C),** Main biological processes affected by rGOT treatment that could mediate the neuroprotective effect of the therapy. LC-MS/MS, liquid chromatography with tandem mass spectrometry; rGOT, human recombinant form of GOT1; tMCAO, transient intra-filament occlusion of the middle cerebral artery. BioRender (<https://biorender.com/>) was used for creating the figures.

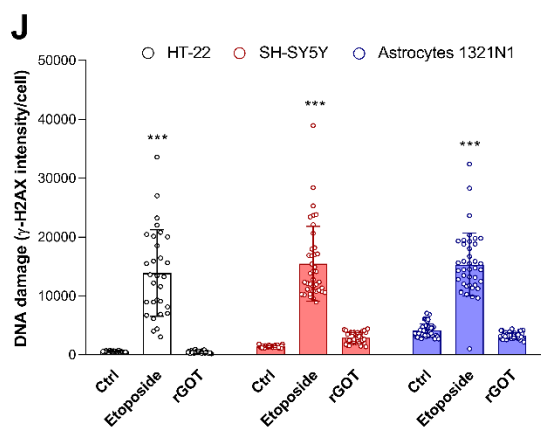
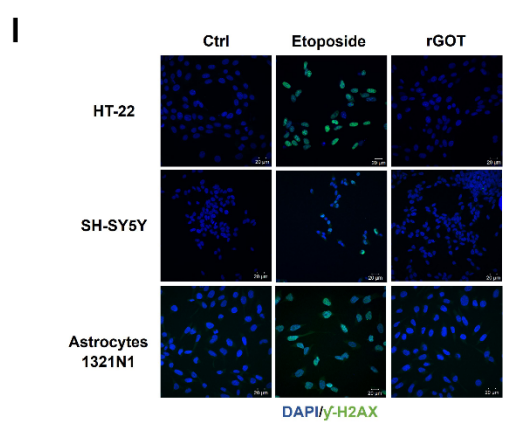
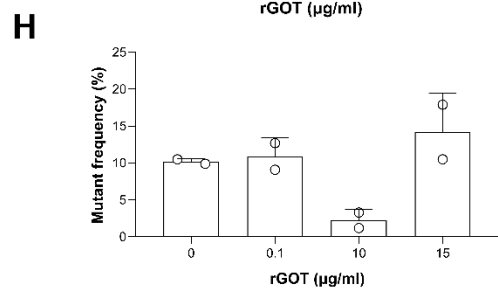
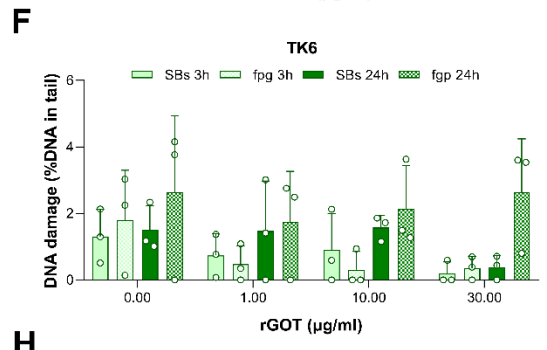
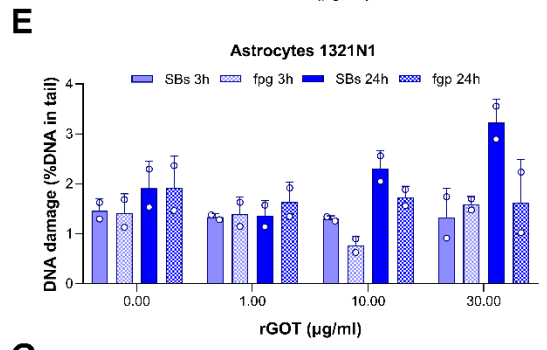
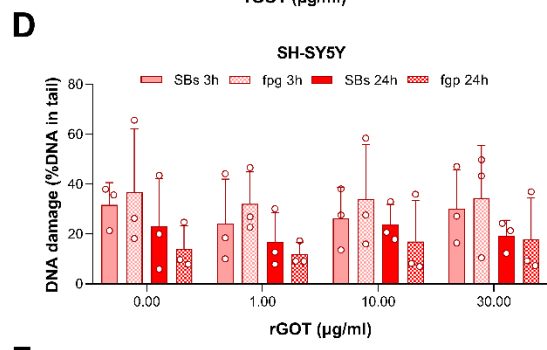
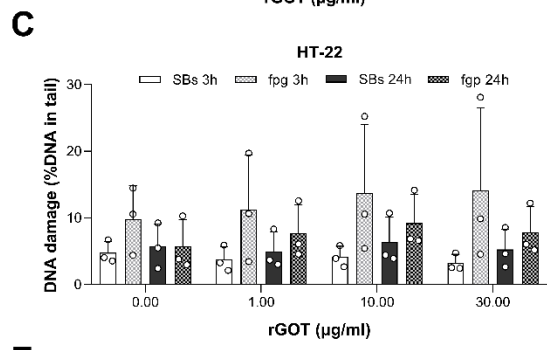
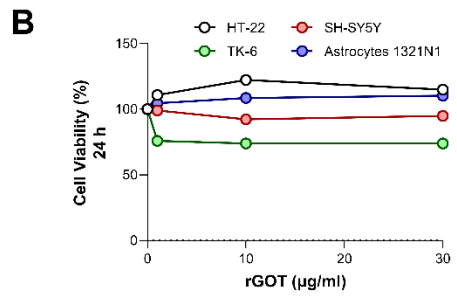
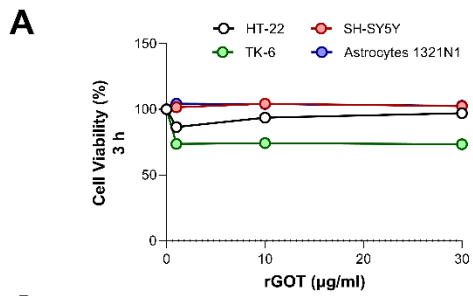


Figure S11. *In vitro* cytotoxic and genotoxic analysis of rGOT, Related to Figure 7. (A), Cells viability of HT-22, SH-5YSY, TK6 and 1321N1 after rGOT exposure for 3 or (B), 24 h. Relative cell viability values are expressed as means \pm SD from duplicate exposure in 2-3 independent experiments calculated relative to the negative control (NC) exposed to cell culture media only (set to 100%). As positive control, cells were treated with chlorpromazine hydrochloride (CHL, 50 μ M), leading to 2-10 % viability (data not shown). One-way ANOVA followed by Bonferroni's multiple comparison test used. No statistically significant differences were observed in response to rGOT compared to untreated cells in any of the cell lines tested. h, hours. (C), DNA damage measured as DNA strand breaks (SBs) and DNA oxidised DNA bases (fpg) measured by the enzyme-linked version of the comet after exposure to rGOT for 3 h or 24 h, respectively in HT-22 (D), SH-5YSY, (E) TK6 and (F) 1321N1. Three independent experiments were performed with duplicate gels for each exposure. DNA damage is expressed as % DNA in tail. The results are shown as mean of the median of duplicate gels from each of the three experiments \pm SD. In all four cell lines, the DNA damage induced by positive control for SBs (H_2O_2 100 μ M) and for Fpg sites (Ro19-8022 2 μ M) was (60-90) and (50-56) % DNA in tail respectively (data not shown). One-way ANOVA followed by Bonferroni's multiple comparison test was used. No statistically significant differences were observed in response to rGOT compared to untreated cells in any of the cell lines tested. h, hours. (G), Chromosomal damage detection using the *in vitro* CBMN assay after exposure of TK6 cells to rGOT for 24 h. The chromosomal damage was expressed as the frequency of Micronuclei (Mn) per binucleated (BN) scored cells (%Mn/BN). Cytotoxicity as cellular proliferation was evaluated using the cytokinesis block proliferation index (CBPI). No induction of chromosomal damage was measured after exposure to rGOT compared to negative control. Mitomycin MMC (0.5 μ g/ml, 4 hours) was used as positive control (9.65 % Mn/BN) compared to negative control (1.83 % Mn/BN) (data not shown). Data are presented as the average value of two independent experiments \pm standard deviation. One-way ANOVA followed by Bonferroni's multiple comparison test. No statistically significant differences were observed in response to rGOT compared to untreated cells. h, hours. (H), Effects of rGOT on induction of HPRT gene mutations after exposure of V79-4 cells to different concentrations for 24 h. The mutant frequency was calculated per 10^6 harvested cells. Each replicate with two independent harvests. Methyl methane sulfonate (MMS, 100 μ M, 3 h) was used as a positive control and induced (40 Mutant per 10^6 viable harvested cells) compared to negative control (10.2 Mutants per

10⁶ viable harvested cells). Data are expressed as the average value of two replicates ± standard deviation. One-way ANOVA followed by Bonferroni's multiple comparison test. Statistically significant differences were observed in response to rGOT compared to untreated cells. h, hours.

(I), Genotoxicity assessment of rGOT using γ -H2AX staining. Representative images of γ -H2AX fluorescent signal in hippocampal cell HT-22, human neuroblastoma SH-5YSY cell, and human astrocytes 1321N1 cells lines after 24 h of exposure to rGOT (30 μ g/ml), negative control (cell culture medium), and positive control Etoposide (20 μ M). Blue represents nuclear staining by DAPI, and green represents γ -H2AX signal.

(J), Quantification of fluorescent signal by GFP intensity of the γ -H2AX signal using ZEN blue software, in HT-22, SH-5YSY and 1321N1 cells. Data are expressed as the average value of two independent experiment replicates ± standard deviation. One-way ANOVA followed by Bonferroni's multiple comparison test. ****p < 0.001*; h, hours. The data were analyzed using SPSS statistical software (v19.0) and GraphPad Prism software (v.8.3.0) for representation of graphs.

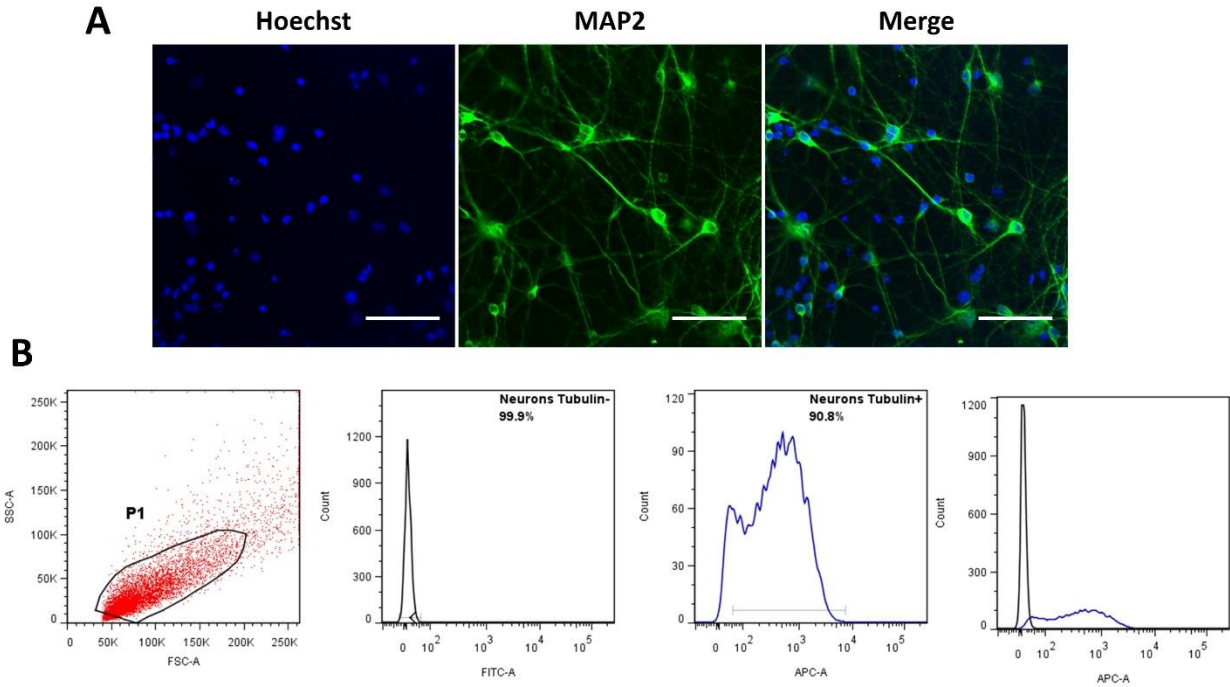


Figure S12. Characterization of the cortical neuron primary cultures, Related to Figure 7.

(A), Immunofluorescence study of the culture using neuronal-specific marker (MAP 2) showed the presence of neurons in the culture. Hoechst: Nucleus staining. Scale bar: 50 μm . (B), Cell phenotype analysis by flow cytometry. Cells positioned in the gate P1 were included for analysis. Unlabeled neurons were used as a negative control (Neurons Tubulin-). The percentage of positive cells for beta-III Tubulin APC antibody was 90.8% (Neurons Tubulin+). On the histograms, the specific staining from Tubulin is shown in blue, whereas the unstained auto fluorescence is the black curve.

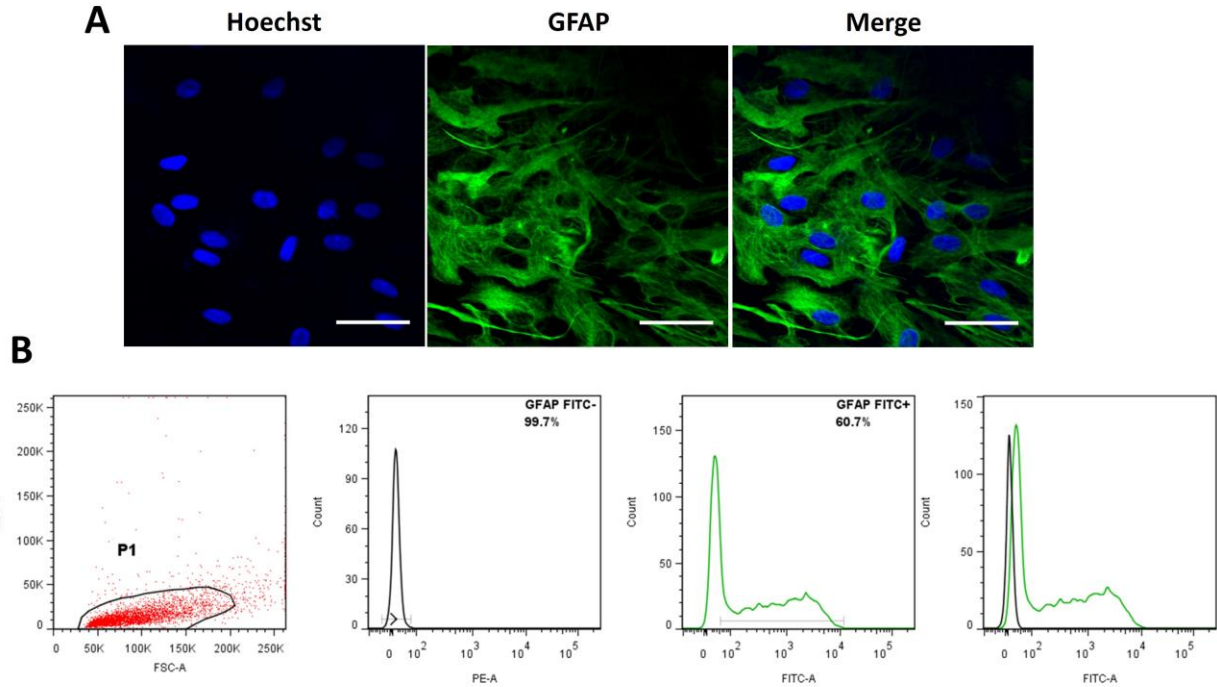


Figure S13. Characterization of the astrocyte primary cultures, Related to Figure 7. (A), Immunofluorescence study of the culture using astrocyte-specific marker (GFAP) showed the presence of astrocytes in the culture. Hoechst: Nucleus staining. Scale bar: 50 μm . **(B),** Cell phenotype analysis by flow cytometry. Cells positioned in the gate P1 were included for analysis. Unlabeled astrocytes were used as a negative control (GFAP FITC-). The percentage of positive cells for GFAP FITC antibody was 60.7% (GFAP FITC+). On the histograms, the specific staining from GFAP is shown in green, whereas the unstained auto fluorescence is the black curve.

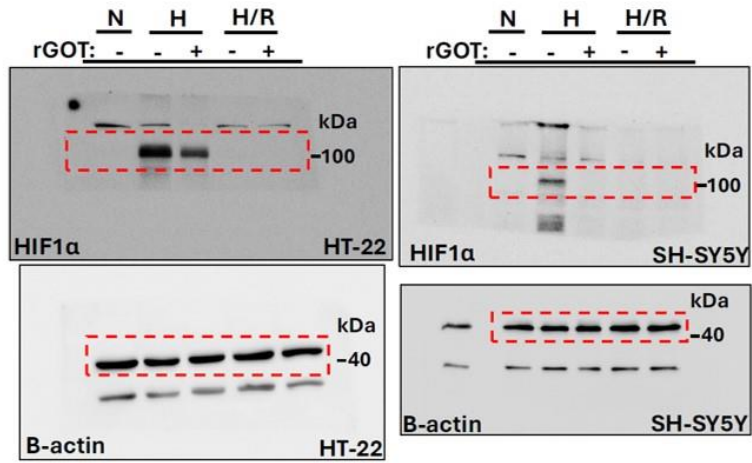
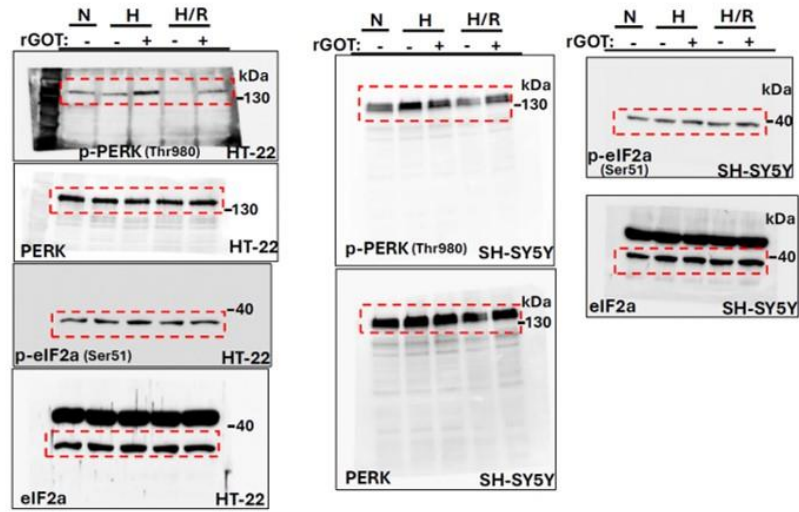
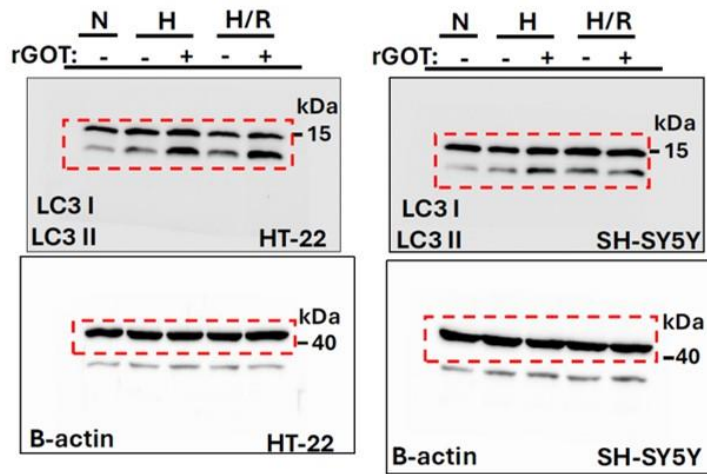
A**B****C**

Figure S14. Full Western blots (WB) images, Related to Figure 8. (A), WB images corresponding to the Figure A. **(B),** WB images corresponding to the Figure D. **(C),** WB images corresponding to the Figure H.

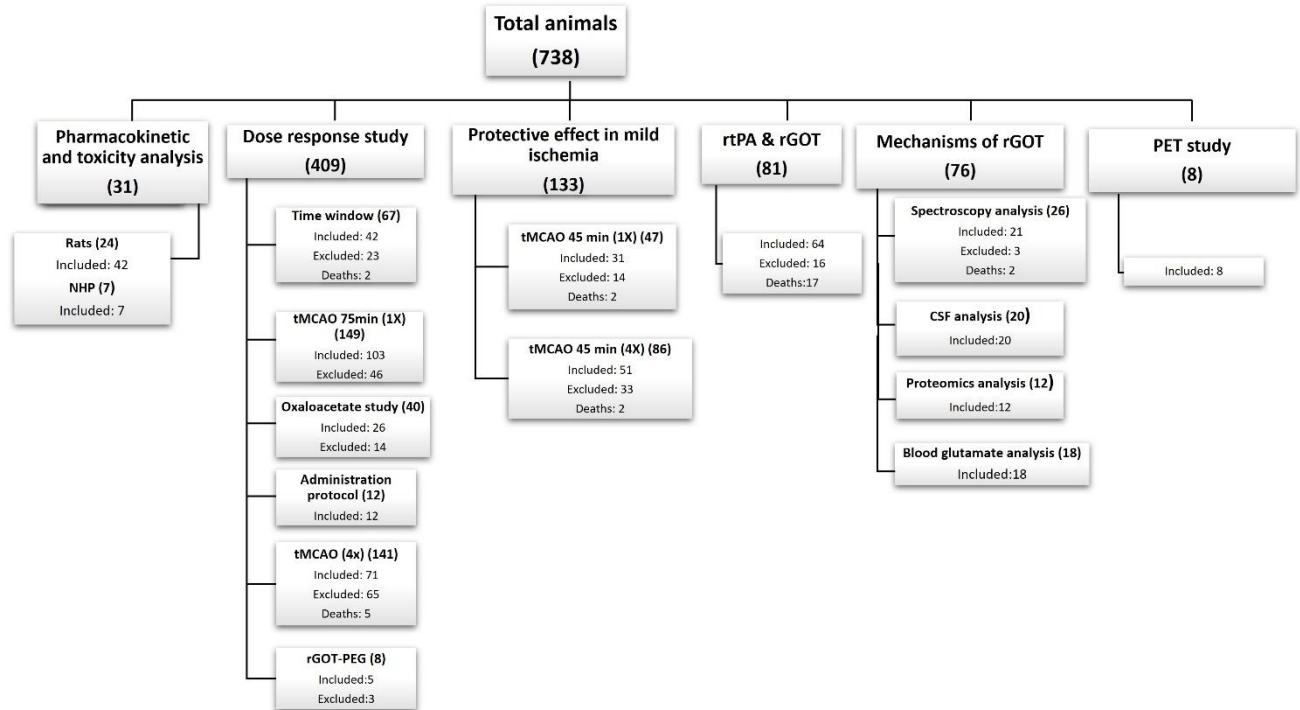


Figure S15. Protocol diagram summarizing the number of animals included and excluded per group, Related to Figures 1-6 and STAR Methods. NHPs, non-human primates; rtPA, recombinant tissue plasminogen activator; rGOT, human recombinant form of glutamate-oxaloacetate transaminase 1; tMCAO, transient middle cerebral artery occlusion; rGOT-PEG, rGOT modified with polyethylene glycol.

SUPPLEMENTARY TABLES

Table S1, Related to Figure 1: Hematological parameters analyzed in non-human primate models.

HEMATOLOGICAL PARAMETERS	
Neutrophils (N)	Mean corpuscular hemoglobin concentration (MCHC)
Eosinophils (E)	Mean corpuscular hemoglobin (MCH)
Basophils (B)	Platelet count (PLT)
Lymphocytes (L)	Mean platelet volume (MPV)
Monocytes (M)	Mean platelet component (MPC)
Red blood cell (RBC) count	Large unstained cells (LUC)
White blood cell (WBC) count	Reticulocytes % (RET%)
Hemoglobin concentration (Hb)	Reticulocytes (RET)
Hematocrit (PCV)	Reticulocyte hemoglobin content (CHr)
Red cell distribution width (RDW)	Reticulocyte mean cell volume (MCVr)
Mean corpuscular volume (MCV)	

Table S2, Related to Figure 1: Biochemical parameters analyzed in non-human primate models.

BIOCHEMICAL PARAMETERS	
Albumin (ALB)	Gamma glutamyl transferase (GGT)
Globulin (GLOB)	Glutamate dehydrogenase (GDH)
Ratio of albumin/globulin (A/G ratio)	Alkaline phosphatase (ALP)
Total bilirubin (T. BILI)	Aspartate aminotransferase (AST)
Calcium (Ca)	Alanine aminotransferase (ALT)
Cholesterol (Chol)	Phosphorus (PHOS)
Creatinine (CREAT)	Total protein (T. PROT)
Glucose (GLU)	Sodium (Na)
Triglycerides (TRIG)	Potassium (K)
Urea	Chloride (Cl)

Table S3, Related to Figure 1: Hemostasis parameters analyzed in non-human primate models.

HEMOSTASIS PARAMETERS
Fibrinogen
Prothrombin (PT)
Activated cephalin time (ACT)

Table S4, Related to Figure 1. Urine parameters analyzed in non-human primate models.

URINE PARAMETERS
Total bilirubin (T. BILI)
Protein urinaire (P. Urinaire)

Table S5, Related to Figure 1. Hematological data: white blood cells (WBCs), red blood cells (RBCs), hemoglobin concentration (HGB), hematocrit (HCT), mean corpuscular volume (MCV), mean corpuscular hemoglobin (MCH), mean corpuscular hemoglobin concentration (MCHC), platelet count (PLT), and reticulocytes (RET).

ANIMAL ID	Timepoint Day (D)	WBC (10³/mm³)	RBC (10⁶/mm³)	HGB (g/dL)	HCT (%)	MCV (μm³)	MCH (pg)	MCHC (g/dL)	PLT (10³/mm³)	RET (%)
Animal 1	D 0	13.8	6.8	14.5	47.7	70.5	21.4	30.4	238	0.3
	D 1	16.4	6.4	13.5	46.0	71.9	21.1	29.3	268	0.5
	D 7	14.9	6.3	13.9	44.1	70.1	22.1	31.5	334	0.5
	D 14	8.4	6.4	13.8	45.2	70.4	21.5	30.5	313	0.3
	D 15	16.8	5.8	12.7	41.2	71.2	21.9	30.8	290	0.3
	D 21	16.4	6.3	13.5	46.2	72.9	21.3	29.2	274	0.6
	D 42	8.5	6.7	14.6	47.1	70.1	21.7	31.0	313	0.3
Animal 2	D 0	13.7	6.9	14.6	47.0	68.5	21.3	31.1	220	0.3
	D 1	14.9	6.5	13.8	45.2	70.1	21.4	30.5	216	0.4
	D 7	9.5	6.4	13.5	43.5	68.3	21.2	31.0	288	0.5
	D 14	7.0	6.4	13.4	43.9	68.7	21.0	30.5	270	0.2
	D 15	12.7	6.1	13.0	42.4	69.2	21.2	30.7	334	0.2
	D 21	11.5	6.4	13.4	44.1	69.0	21.0	30.4	227	0.4
	D 42	9.8	6.6	13.7	45.2	68.8	20.9	30.3	239	0.4
Animal 3	D 0	7.5	7.6	15.0	47.9	63.1	19.8	31.3	336	0.4
	D 1	7.9	7.1	14.0	45.9	64.9	19.8	30.5	247	0.3
	D 7	6.4	7.2	14.2	45.1	62.7	19.7	31.5	276	0.7
	D 14	8.7	7.2	14.3	46.0	64.0	19.9	31.1	90	0.5
	D 15	13.5	6.7	13.3	42.7	63.9	19.9	31.1	252	0.5
	D 21	11.9	7.1	13.8	44.9	63.3	19.5	30.7	304	0.6

	D 42	7.1	7.4	14.5	46.0	62.3	19.6	31.5	634	0.3
Animal 4	D 0	11.8	7.7	16.0	51.3	66.5	20.7	31.2	124	0.3
	D 1	8.2	6.7	13.9	45.9	68.9	20.9	30.3	207	0.6
	D 7	8.8	6.9	14.5	46.6	67.2	20.9	31.1	386	0.6
	D 14	7.2	6.9	14.5	46.5	67.4	21.0	31.2	220	0.4
	D 15	7.7	6.6	13.8	45.0	68.5	21.0	30.7	212	0.4
	D 21	6.4	6.6	13.7	45.3	69.1	20.9	30.2	246	0.6
	D 42	10.5	7.4	15.1	50.0	67.9	20.5	30.2	212	0.5

Table S6, Related to Figure 1. Leukocyte differential count results: white blood cells (WBCs), neutrophils (NEUs), lymphocytes (LYMs), monocytes (MONs), eosinophils (EOSs), and basophils (BASs).

ANIMAL ID	Timepoint Day (D)	WBC (10³/m³)	NEU (10³/mm³)	LYM (10³/mm³)	MON (10³/mm³)	EOS (10³/mm³)	BAS (10³/mm³)	NEU (%)	LYM (%)	MON (%)	EOS (%)	BAS (%)
Animal 1	D 0	13.8	10.3	2.4	0.6	0.2	0.4	74.4	17.1	4.1	1.6	2.8
	D 1	16.4	9.5	5.6	0.9	0.4	0	58.0	34.1	5.4	2.3	0.2
	D 7	14.9	10.8	2.8	0.6	0.6	0	72.5	19.0	4.1	4.2	0.2
	D 14	8.4	3.0	4.2	0.6	0.5	0.1	35.7	50.4	7.6	5.5	0.8
	D 15	16.8	11.4	4.3	0.6	0.5	0	68.0	25.4	3.8	2.7	0.1
	D 21	16.4	11.0	3.5	0.7	1.2	0	67.0	21.1	4.2	7.5	0.2
	D 42	8.5	4.4	3.4	0.5	0.1	0	52.1	40.5	5.7	1.5	0.2
Animal 2	D 0	13.7	8.8	3.7	1.0	0.1	0.1	64.2	27.2	7.2	0.8	0.6
	D 1	14.9	7.2	6.4	1.0	0.3	0.1	48.5	43.0	6.4	1.7	0.4
	D 7	9.5	5.4	3.2	0.7	0.1	0.1	57.2	34.1	6.9	1.3	0.5
	D 14	7.0	2.5	3.7	0.6	0.1	0	36.4	53.7	8.2	1.1	0.6
	D 15	12.7	5.8	5.7	0.9	0.3	0.1	45.7	44.5	6.8	2.5	0.5
	D 21	11.5	7.7	3.1	0.7	0	0	66.6	27.0	5.8	0.3	0.3
	D 42	9.8	4.3	4.4	1.0	0.1	0.1	43.4	44.7	10.0	1.3	0.6
Animal 3	D 0	7.5	2.7	4.2	0.5	0.2	0	35.4	55.8	6.3	2.0	0.5
	D 1	7.9	2.1	5.1	0.3	0.3	0	27.0	64.8	4.1	3.7	0.4
	D 7	6.4	2.5	3.5	0.3	0.1	0	39.7	54.5	4.4	1.1	0.3
	D 14	8.7	2.7	5.3	0.3	0.3	0	31.0	61.0	4.0	4.0	0
	D 15	13.5	6.2	6.3	0.6	0.4	0.1	45.5	46.3	4.6	3.2	0.4
	D 21	11.9	6.8	4.3	0.5	0.2	0	57.2	36.2	4.6	1.8	0.2

	D 42	7.1	1.5	5.1	0.4	0.1	0.1	21.5	71.2	5.2	1.4	0.7
Animal 4	D 0	11.8	6.5	4.2	1.0	0	0.1	55.5	35.6	8.2	0.2	0.5
	D 1	8.2	1.7	5.6	0.8	0.1	0	20.6	68.1	9.8	1.1	0.4
	D 7	8.8	4.0	4.2	0.5	0	0	45.3	48.1	5.9	0.2	0.5
	D 14	7.2	1.1	5.2	0.8	0.1	0.1	14.7	72.2	10.9	1.5	0.7
	D 15	7.7	1.7	5.2	0.6	0.1	0	22.6	67.7	8.3	0.9	0.5
	D 21	6.4	2.1	3.6	0.7	0.1	0	33.0	55.3	10.1	1.1	0.5
	D 42	10.5	2.2	7.3	1.0	0	0.1	20.4	69.4	9.3	0.3	0.6

Table S7, Related to Figure 1. Hemostasis data: prothrombin (PT), activated cephalin time (ACT), and fibrinogen (FIG).

ANIMAL ID	Time-point (d)	PT (s)	ACT (s)	FIG (g/L)
Animal 1	D 0	14.0	24.5	2.26
	D 1	13.9	27.4	2.17
	D 7	14.9	29.5	2.34
	D 14	13.1	25.3	1.86
	D 15	13.0	23.4	2.04
	D 21	13.1	26.1	2.23
	D 42	14.0	28.0	1.44
Animal 2	D 0	13.3	25.0	2.30
	D 1	12.6	21.9	2.37
	D 7	13.8	26.6	2.36
	D 14	12.9	25.3	2.01
	D 15	13.1	24.1	2.08
	D 21	13.1	24.8	2.20
	D 42	13.8	25.8	1.93
Animal 3	D 0	14.4	27.1	2.55
	D 1	12.5	23.7	2.32
	D 7	13.7	25.6	2.42
	D 14	12.8	22.6	2.44
	D 15	12.9	23.0	2.40
	D 21	13.0	24.4	2.33
	D 42	12.9	24.2	1.53
Animal 4	D 0	12.9	24.6	2.37
	D 1	12.9	24.8	2.27

	D 7	13.5	27.0	2.22
	D 14	12.9	27.5	1.79
	D 15	13.5	26.2	1.88
	D 21	12.7	27.1	2.21
	D 42	14.6	30.6	1.40

Table S8, Related to Figure 1. Biochemical data I: albumin (ALB), glutamate pyruvate transaminase (GPT), glutamate oxaloacetate transaminase (GOT), calcium (Ca), cholesterol (Chol), creatinine (CREAT), gamma-glutamyl transferase (GGT), glutamate dehydrogenase (GDH), glucose (GLU), and chloride (Cl).

ANIMAL ID	Timepoint Day (D)	ALB (g/L)	GPT (U/L)	GOT (U/L)	Ca (mM)	Chol (mM)	CREAT (mM)	GGT (U/L)	GDH (U/L)	GLU (mM)	Cl (mM)
Animal 1	D 0	42	58	65	2.81	2.5	71	147	19.6	3.8	121
	D 1	50	82	2295	2.71	2.6	81	151	18.3	7.3	112
	D 7	49	78	98	2.63	2.6	72	131	12.8	4.7	108
	D 14	53	50	51	2.77	2.4	72	138	12.0	5.8	113
	D 15	48	79	14082	2.59	2.1	70	126	18.6	6.1	113
	D 21	50	64	257	2.71	2.6	88	129	16.7	5.6	118
	D 42	51	234	74	2.90	2.9	82	212	76.3	4.5	117
Animal 2	D 0	42	88	88	2.74	2.1	75	276	29.6	4.9	124
	D 1	42	106	1786	2.71	2.2	66	261	24.9	4.3	109
	D 7	49	100	122	2.67	2.5	75	269	22.1	3.9	109
	D 14	44	79	58	2.62	2.3	64	244	21.3	5.5	112
	D 15	43	93	101105	2.46	2.3	66	225	23.0	5.2	111
	D 21	47	85	266	2.62	2.2	69	218	16.0	3.4	117
	D 42	44	212	65	2.71	2.5	94	255	59.9	5.3	113
Animal 3	D 0	40	46	42	2.49	2.4	76	125	17.3	3.6	121
	D 1	41	54	1639	2.57	2.5	73	117	14.9	3.3	111
	D 7	44	42	60	2.46	2.5	67	122	13.0	3.4	110
	D 14	43	45	45	2.57	2.5	74	126	17.2	5.2	111
	D 15	40	52	9979	2.40	2.2	71	115	17.8	3.8	112
	D 21	44	55	104	2.51	2.2	75	128	23.2	2.7	116

	D 42	44	185	56	2.59	2.9	81	246	36.4	4.3	117
Animal 4	D 0	43	73	50	2.97	2.2	63	146	46.7	4.2	122
	D 1	44	84	1590	2.66	2.5	55	145	42.2	4.5	111
	D 7	49	68	109	2.72	2.5	64	164	30.2	4.2	112
	D 14	49	67	62	2.73	2.4	52	170	45.7	6.3	116
	D 15	49	66	7441	2.54	2.2	65	159	32.4	6.7	113
	D 21	52	54	200	2.73	2.5	64	157	32.3	4.5	116
	D 42	48	219	73	2.82	2.6	61	237	118	3.9	117

Table S9, Related to Figure 1. Biochemical data I: potassium (K), sodium (Na), alkaline phosphatase (ALP), phosphorus (PHOS), total protein (T PROT), triglycerides (TRIG), globulin (GLOB), and albumin/globulin (A/G ratio).

ANIMAL ID	Timepoint Day (D)	K (mM)	Na (mM)	ALP (U/L)	PHOS (mM)	T PROT (g/L)	TRIG (mM)	UREA (mM)	GLOB (g/L)	A/G Ratio
Animal 1	D 0	4.4	165	1186	1.74	84	0.36	7.3	41	1.0
	D 1	4.0	157	1020	1.82	80	0.58	5.6	30	1.7
	D 7	3.5	151	1119	2.11	84	0.36	6.3	35	1.4
	D 14	4.2	154	944	1.47	79	0.73	7.5	26	2.0
	D 15	3.9	150	850	1.22	83	1.03	8.4	35	1.4
	D 21	3.0	162	923	1.42	85	0.65	9.1	35	1.4
	D 42	5.1	160	954	2.14	86	0.52	5.7	35	1.5
Animal 2	D 0	4.6	166	1222	1.37	74	0.40	11.0	32	1.3
	D 1	4.0	151	927	1.34	72	0.50	7.1	30	1.4
	D 7	3.9	148	1283	2.19	77	0.52	8.6	28	1.8
	D 14	4.2	151	992	1.82	71	0.37	6.7	27	1.6
	D 15	3.3	148	880	1.38	80	0.58	9.4	37	1.2
	D 21	4.0	157	947	1.78	78	0.45	10	31	1.5
	D 42	3.3	157	823	2.25	80	0.84	8.2	36	1.2
Animal 3	D 0	3.9	164	297	1.34	76	0.40	9.0	36	1.1
	D 1	4.2	154	1055	1.21	74	0.55	7.3	33	1.2
	D 7	3.4	148	1316	1.75	74	0.49	9.2	30	1.5
	D 14	3.7	154	1031	1.60	73	0.52	9.6	30	1.4
	D 15	3.2	150	920	1.16	74	0.69	9.4	34	1.2
	D 21	3.0	154	1169	1.76	77	0.50	10.2	33	1.3
	D 42	3.2	156	1274	2.22	77	0.80	8.1	33	1.3

Animal 4	D 0	4.9	173	616	1.90	82	0.50	11.0	39	1.1
	D 1	4.3	157	572	1.12	75	1.17	6.8	31	1.4
	D 7	4.2	156	768	2.36	82	0.35	8.9	33	1.5
	D 14	4.8	157	574	1.88	75	0.73	7.0	26	1.9
	D 15	3.9	153	618	2.01	82	1.15	6.5	33	1.5
	D 21	4.0	157	651	1.67	86	0.96	9.3	34	1.5
	D 42	3.6	161	769	2.72	82	0.55	7.2	34	1.4

Table S10, Related to Figure 1. Urinalysis data: total bilirubin (T. BILI) and protein urinary (P. Urinaire).

ANIMAL ID	Timepoint Day (D)	T. BILI (μM)	P. Urinaire (g/L)
Animal 1	D 0	3.3	0.37
	D 1	3.4	ND*
	D 7	3.4	<0.08
	D 14	2.1	<0.08
	D 15	2.2	ND*
	D 21	1.9	0.09
	D 42	3.2	NA*
Animal 2	D 0	4.7	0.26
	D 1	3.4	ND*
	D 7	5.6	0.13
	D 14	2.9	<0.08
	D 15	3.3	ND*
	D 21	4.5	<0.08
	D 42	4.9	ND*
Animal 3	D 0	2.9	0.08
	D 1	1.9	ND*
	D 7	3.5	<0.08
	D 14	2.1	<0.08
	D 15	2.2	ND*
	D 21	2.6	0.1
	D 42	3.6	ND*
Animal 4	D 0	3.1	0.14
	D 1	2.3	ND*

	D 7	3.7	0.08
	D 14	2.1	<0.08
	D 15	1.7	ND*
	D 21	2.4	<0.08
	D 42	3.1	NA*

*ND; no data available